Sensors and Actuators A 250 (2016) 195–201

Contents lists available at ScienceDirect

Sensors and Actuators A: Physical

journal homepage: www.elsevier.com/locate/sna

Error-separation method for the calibration of magnetic compass

Zhiwei Chu[a,b,c], Xinhua Lin[a,b,*], Ke Gao[a,b,c], Chilai Chen[a,b]

[a] The State Key Laboratory of Transducer Technology, Institute of Intelligent Machines, Chinese Academy of Sciences, Hefei 230031, China
[b] Department of Automation, School of Information Science and Technology, University of Science and Technology of China, Hefei 230026, China
[c] The Key Laboratory of Biomimetic Sensing and Advanced Robot Technology of Anhui Province, Institute of Intelligent Machines, Chinese Academy of Sciences, Hefei 230031, China

ARTICLE INFO

Article history:
Received 23 November 2015
Received in revised form 17 August 2016
Accepted 19 September 2016
Available online 20 September 2016

Keywords:
Magnetic compass
Calibration
Error separation
Non-magnetic platform

ABSTRACT

Magnetic compass is widely used in the navigation system by measuring the orientation of the earth's magnetic field and must be calibrated before used to eliminate the errors caused by the bias, misalignment, inconsistence in sensitivity, etc. In this paper, the fully digital magnetic compass was developed by using magnetic-induced magnetometers and MEMS accelerometers and the error-separation method based on a non-magnetic three-axis rotation platform was presented to calibrate the magnetic compass. The parameters about misalignment and non-orthogonality of the sensor axes and the response curve of the sensor's output signals to earth magnetic fields were obtained. Furtherly, the sensitivity of magnetometers and the bias from the offset and hard-magnetic interference were estimated according to the response curve. The independent effect of non-orthogonality and misalignment, bias and inconsistence in sensitivity on the heading error can be evaluated with the error-separation method, respectively. After calibration, the maximum heading error of magnetic compass was about 0.4° when both pitch angle and roll angle were in the range from −60° to 60°, indicating the error-separation method is effective and efficient to calibrate magnetic compasses.

1. Introduction

The magnetic compass is a device that can determine the orientation of earth magnetic field, i.e. heading information and is generally used in wide fields of applications from navigation systems for cars, ships, robots and aircrafts to drilling systems due to its advantage of no error accumulation. Besides magnetic sensors, the magnetic compass usually contains acceleration sensors that are used to achieve the attitude compensation by measuring the actual roll and pitch angles of the magnetic compass [1,2]. But only attitude compensation is not enough to obtain the heading orientation with high precision since the deviations in biases and scale factor of magnetic sensors and misalignment and non-orthogonality of the sensor axes can distort the output of magnetic compass. In addition, local magnetic interferences like hard iron and soft iron interferences can also disturb the magnetic compass. Thus, magnetic compass must be calibrated before used and various calibration procedures and algorithms have been reported [2–8]. Caruso exploited the output minimum and maximum value obtained from the magnetic sensor on a horizontal rotating platform to estimate the scale factors and biases [3]. In this calibration method, several errors like the non-orthogonality of the sensor axes were not taken into account. In the reference [2], a digital magnetic compass based on AMR magnetometers and MEMS accelerometers was developed and a called scalar calibration was reported. The errors of bias, inconsistence in sensitivity, non-orthogonality, and misalignment were estimated by applying an iteration algorithm to data sets obtained from accelerometers and magnetometers. Gebre-Egziabher et al. proposed a more complete calibration algorithm to fit an ellipsoid of revolution to measured magnetic field data by using an iterative batch least squares estimator [4]. After calibration, the heading errors were just on the order of 1°–2° due to the neglect of misalignment errors. Wang employed the neural network algorithms to calibrate the compass by modeling the nonlinear relationship between the compass heading and the true heading. During training the neural network, an external heading reference was required, which imposes limitation on this neural network method. Without any simplification on the nature of errors, both Fang [6] and Renaudin [7] adopt an ellipsoid fitting algorithm to calibrated magnetic compass. In order to acquire the high heading precision, about several-hundred measurement data of magnetometers in different orientations were usually needed, resulting in a time-consuming task since the more measurements,

* Corresponding author at: The State Key Laboratory of Transducer Technology, Institute of Intelligent Machines, Chinese Academy of Sciences, Hefei 230031, China.
E-mail address: xhlin@iim.ac.cn (X. Lin).

http://dx.doi.org/10.1016/j.sna.2016.09.024
0924-4247/

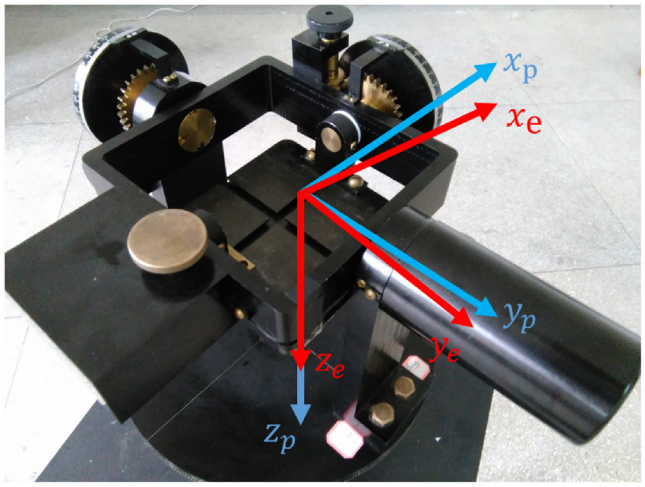

Fig. 1. Photograph of the three-axis rotating non-magnetic platform and Scheme the earth magnetic field frame and the platform frame.

the higher precision. In addition, it was demonstrated that on the existence of soft magnetic disturbance, an ellipsoid fitting algorithm was not an effective method to obtain magnetic compass with small heading errors [7], which meaning it will be better to avoid soft iron interferences as much as possible during the process of calibration and application.

Non magnetic platforms with three rotating axes combined with the method of scalar calibration have been used to calibrate magnetic compasses [3,9,10]. In the procedure of the scalar calibration, an iteration algorithm was usually applied to indirectly determine the best deviation angles by minimizing the dispersion of the earth magnetic field and gravity [3]. In this paper, a similar three-axial nonmagnetic platform was designed and a direct algorithm called as error-separation method, was proposed to calibrate magnetic compasses under the prerequisite that no soft iron disturbance existed. The achievement of high-precise magnetic compasses demonstrated that the calibration algorithm of error separation based on the three-axial nonmagnetic platform was very effective and it was not difficult to avoid or alleviate soft iron interferences in practical application since the magnetic compass was composed of commercial-off-the-shelf components.

2. Hardware implementation and 3D platform

The magnetic compass mainly consisted of a triad of magnetometers and a triad of MEMS accelerometers and had a perfect cuboid frame. The magnetometers work on the principle of magneto-inductance (MI) effects that the inductance of magnetometers is proportional to the external magnetic field [11]. MI magnetometers generally serve as the inductive element in a simple LR relaxation oscillation circuit. The output from this circuit is inherently digital and can be fed into microprocessors directly. The MEMS accelerometers are used to calculate the roll and pitch angles of magnetic compasses. The magnetometers and accelerometers were purchased from the market and were produced by PNI Sensor Corporation and STMicroelectronics, respectively.

The non-magnetic platform has three rotating axes as shown in Fig. 1. Three rotating axes are mutually perpendicular and the error of vertical angler is less than 0.05°. The angle position of each rotating axis was measured by an optoelectronic encoder with the precision of 0.0001°. In order to avoid introducing the magnetic interference as much as possible, the platform was mainly made of non-magnetic materials like aluminum alloy, brass and plastic and, was driven manually instead of with motors.

3. Calibration of magnetometers

3.1. The principle of measurement

First of all, several coordinate frames used thereafter in this paper were defined in Figs. 1 and 2. The coordinate frame (e) is the earth magnetic field frame. The x_e-axis is along the direction of horizontal component of the earth magnetic field vector (H_E). The z_e-axis is in the downward direction. The y_e-axis is in the direction perpendicular to the plane formed by the x_e and z_e and obeys the right-hand rule. The platform frame (p) was also shown in Fig. 1. x_p, y_p and z_p are along the direction of three different rotating axes of platform, respectively. m is the measurement frame, whose three axes are along the sensitive axes of the magnetometer triad and are ordinarily not orthogonal to each other (see Fig. 2). The case body frame of magnetic compass was denoted as the b coordinate frame and has three orthogonal axes of x_b, y_b and z_b. And x_l, y_l and z_l are the axes of the local level frame (l). x_l and y_l lies in the local level plane. z_l is along the direction of gravity. θ and γ are the pitch and roll angles of the body frame (b) relative to the local level frame (l), respectively.

In order to calculate the heading, the measurement in the case body frame (b) must be transformed into that on the local level frame (l) by the following the relationship:

$$\begin{bmatrix} h_x^l \\ h_y^l \\ h_z^l \end{bmatrix} = \begin{bmatrix} \cos\gamma & \sin\gamma\sin\theta & -\sin\gamma\cos\theta \\ 0 & \cos\theta & \sin\theta \\ \sin\lambda & -\sin\theta\cos\gamma & \cos\gamma\cos\theta \end{bmatrix} \begin{bmatrix} h_x^b \\ h_y^b \\ h_z^b \end{bmatrix} \quad (1)$$

Where h_x^l, h_y^l and h_z^l are the components of Earth magnetic field in the direction of the x_l, y_l and z_l axes, respectively, while h_x^b, h_y^b and h_z^b are the components of Earth magnetic field in the axis directions of the body frame (b).

The heading (ψ) is calculated as follows:

$$\phi = arctg\left(\frac{h_x^l}{h_y^l}\right) \quad (2)$$

$$\psi = \begin{cases} \phi, (h_x^l > 0, h_y^l \geq 0) \\ \pi + \phi, (h_x^l < 0) \\ 2\pi + \phi, (h_y^l > 0) \\ \pi/2, (h_x^l = 0, h_y^l > 0) \\ 3\pi/2, (h_x^l = 0, h_y^l < 0) \end{cases} \quad (3)$$

3.2. Error modeling of magnetometers

The measurement made by the magnetometers is often corrupted by instrumentation errors and magnetic deviation [7]. Instrumentation errors include offset error, scale factor error, measurement noise and non-orthogonality error from the imperfection of fabrication and installation. Magnetic deviation can be classified into hard iron errors and soft iron errors. Hard iron errors are generated by a magnetic source with permanent field in all orientations. The permanent field causes a bias in the sensed magnetic field [4]. Soft iron errors result from the kind of ferro-magnetic materials that generate their own magnetic field in response to an externally applied field. This generated magnetic field is affected by both the magnitude and direction of the externally applied magnetic field. It has been proved that soft iron errors are difficult to be eliminated [7] and it is better to avoid soft magnetic materials as soon

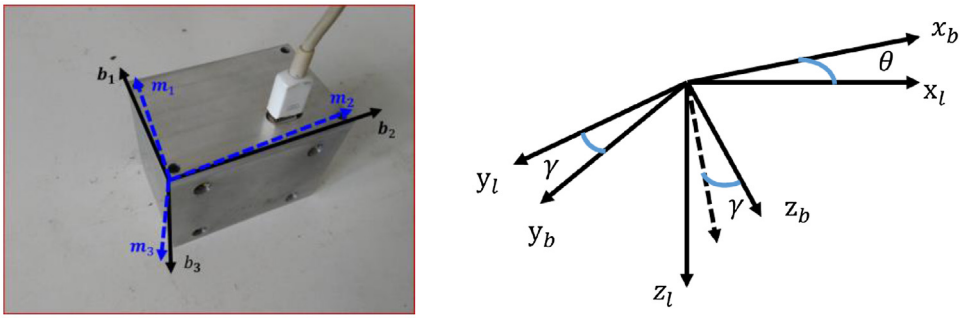

Fig. 2. (a) Photograph of the magnetic compass and Scheme of the measurement frame and the body frame; (b) Relationship between the body frame and the local level frame.

as possible. Thus, in our paper, the error model can be described as follows:

$$\begin{bmatrix} h_x^m \\ h_y^m \\ h_z^m \end{bmatrix} = M_k M_o \begin{bmatrix} h_x^b \\ h_y^b \\ h_z^b \end{bmatrix} + \begin{bmatrix} b_x^m \\ b_y^m \\ b_z^m \end{bmatrix} + \begin{bmatrix} n_x^m \\ n_y^m \\ n_z^m \end{bmatrix} \quad (4)$$

Where h_x^m, h_y^m and h_z^m are the outputs of the magnetometer triad. b_x^m, b_y^m and b_z^m are the combined biases from the offset and hard iron interference that shift the outputs of the magnetometer triad. h_x^b, h_y^b and h_z^b are the true components of the earth magnetic field in the direction of x_b, y_b and z_b. M_k is a 3-D diagonal matrix that accounts for the sensitivities of the triad of magnetometers by scaling the outputs. M_0 is also the 3×3 matrix that accounts for the non-orthogonality and misalignment of the magnetometer triad. n_x^m, n_y^m and n_z^m represent the noises of the magnetometer triads and can be eliminated by averaging the outputs. Then, the above Eq. (4) can be substituted with the following Eq. (5). The main task of calibration is to determine precisely the parameters in the above Eq. (5) and then, to correct the erroneous outputs to get the true magnetic field.

$$\begin{bmatrix} \overline{h_x^m} \\ \overline{h_y^m} \\ \overline{h_z^m} \end{bmatrix} = M_k M_o \begin{bmatrix} h_x^b \\ h_y^b \\ h_z^b \end{bmatrix} + \begin{bmatrix} b_x^m \\ b_y^m \\ b_z^m \end{bmatrix} \quad (5)$$

where $\overline{h_x^m}$, $\overline{h_y^m}$ and $\overline{h_z^m}$ were the average outputs of the magnetometers in the directions of x_m, y_m and z_m axe, respectively, when the measurements were repeated three to five times at the same position.

3.3. Calibration of magnetometers

Firstly, the three-axis rotation platform was adjusted to keep the x_p–y_p plane level, and the body case of magnetic compass was rigidly mounted on the x_p–y_p plane of platform to guarantee the x_b and z_b axes in the body frame aligned with the x_p and z_p axes in the platform frame. Then, the platform was alternatively rotated manually around the axes of x_p, y_p and z_p to obtain the deviation angles between the axes of the measurement frame (m) and the axes of the body frame (b) by determining the angle positions at which the magnetometers had the maximum outputs. As a result, the relation between m and b was expressed as the following:

$$\begin{bmatrix} x_m \\ y_m \\ z_m \end{bmatrix} = \begin{bmatrix} \cos\angle x_m x_b & \cos\angle x_m y_b & \cos\angle x_m z_b \\ \cos\angle y_m x_b & \cos\angle y_m y_b & \cos\angle y_m z_b \\ \cos\angle z_m x_b & \cos\angle z_m y_b & \cos\angle z_m z_b \end{bmatrix} \begin{bmatrix} x_b \\ y_b \\ z_b \end{bmatrix} \quad (6)$$

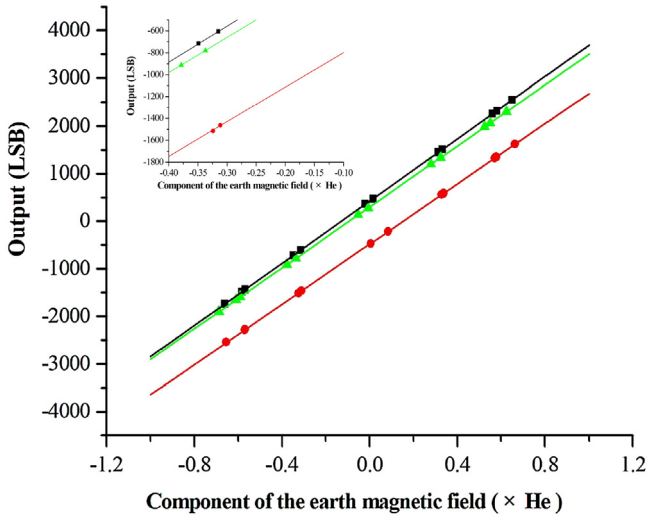

Fig. 3. Fitted curves between the output of magnetomters and the component of the earth magnetic field in the direction of the magnetic sensor axes (x_m axis: —, y_m axis: — , and z_m axis: —) and the original outputs of magnetometers (x_m axis: ■, y_m axis: ● and z_m axis: ▲); H_e equal to the magnitude of the earth magnetic field.

where $\angle i_m j_b$ (i = x, y or z; j = x, y or z) was the angle between one axis in m frame and one axis in b frame.

At the same time, the angle (δ) between the x_p axis and the horizontal component of the indoor magnetic field vector and the angle (ϕ) between the x_p–y_p plane and the indoor magnetic field were acquired with the similar procedure when the x_p–y_p plane was kept level. Here, δ and ϕ were called as the declination angle and inclination angle, respectively. Now, When the platform was rotated around the axis of z_p to the angle of α, the true component of the earth magnetic field vector on the x_m axis of the measurement frame (m) can be calculated as follows:

$$H_x^m = [\cos\angle x_m x_b \cos\phi\cos(\alpha - \delta) + \cos\angle x_m y_b \cos\phi \sin(\alpha - \delta) + \cos\angle x_m z_b \sin\phi] H_e \quad (7)$$

Where H_x^m represented the true component of the earth magnetic field vector on the x_m axis. H_e was the earth magnetic field vector. When the platform was rotated around the axis of z_p in the range of $\pm 180^\circ$, a data set of outputs in the direction of x_m axis were obtained. By fitting the set of data with the method of least square, the function of output on the true component of earth magnetic field was acquired. Since MI magnetometers show a linear response to the magnetic field in the range of earth magnetic field [11], the function can be written as follows:

$$\overline{h_x^m} = k_x^m H_x^m + b_x^m \quad (8)$$

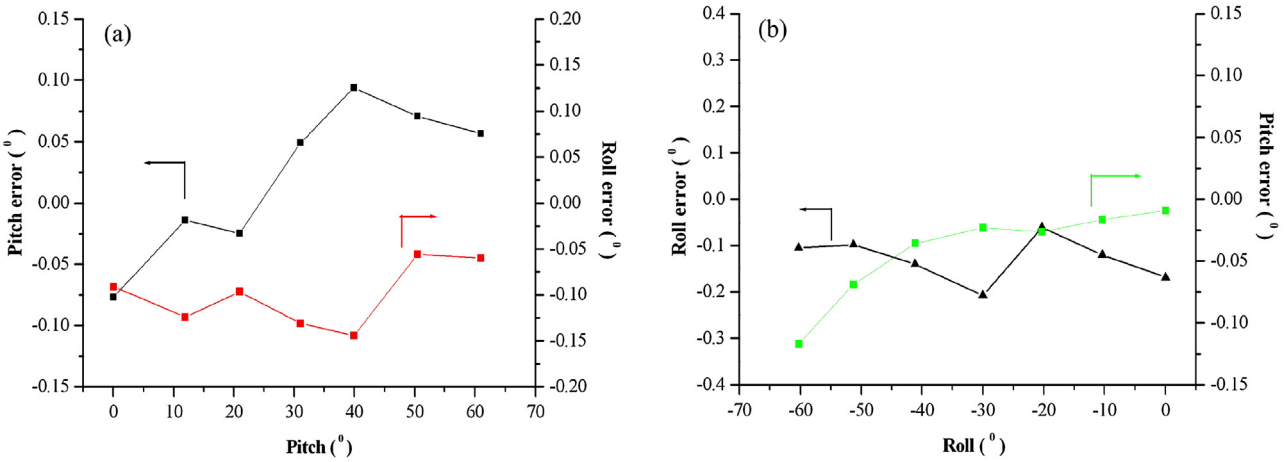

Fig. 4. Pitch and Roll errors, (a) the roll angle kept at 20°; (b) the pitch angle kept at 20°.

Where k_x^m and b_x^m were the sensitivity and combined bias of the magnetometer in the direction of x_m axis, respectively, which were directly obtained from the slope and intercept of the fitting response curve of the average output to the true component of the earth magnetic field in the direction of x_m axis. Similarly, two data sets of the other two average outputs in the directions of y_m and z_m axes were fitted and correspondingly, k_y^m, k_z^m, b_y^m and b_z^m were also obtained. By combining the Eqs. (4), (6) and (8), two 3 × 3 matrices of M_k and M_0 were inferred and were written as the following:

$$M_o = \begin{bmatrix} \cos\angle x_m x_b & \cos\angle x_m y_b & \cos x_m z_b \\ \cos\angle y_m x_b & \cos\angle y_m y_b & \cos\angle y_m z_b \\ \cos\angle z_m x_b & \cos\angle z_m y_b & \cos\angle z_m z_b \end{bmatrix} \tag{9}$$

$$M_k = \begin{bmatrix} k_x^m & 0 & 0 \\ 0 & k_y^m & 0 \\ 0 & 0 & k_z^m \end{bmatrix} \tag{10}$$

After b_x^m, b_y^m, b_z^m, M_k and M_0 were obtained, the errors from the sensitivity inconsistency, the combined biases, and the non-orthogonality and misalignment can be eliminated independently. According to the Eqs. (4), (6), (9) and (10), the true components of earth magnetic field in the axis directions of the case body frame (b) were formulated as:

$$\begin{bmatrix} h_x^b \\ h_y^b \\ h_z^b \end{bmatrix} = \begin{bmatrix} \cos\angle x_m x_b & \cos\angle x_m y_b & \cos\angle x_m z_b \\ \cos\angle y_m x_b & \cos\angle y_m y_b & \cos\angle y_m z_b \\ \cos\angle z_m x_b & \cos\angle z_m y_b & \cos\angle z_m z_b \end{bmatrix}^{-1} \begin{bmatrix} k_x^m & & \\ & k_y^m & \\ & & k_z^m \end{bmatrix}^{-1} \begin{bmatrix} \overline{h_x^m} - b_x^m \\ \overline{h_y^m} - b_y^m \\ \overline{h_z^m} - b_z^m \end{bmatrix}. \tag{11}$$

Table 1
Deviation angles between the axes of the measurement frame and of the body frame.

$\angle x_m x_b$	$\angle x_m y_b$	$\angle x_m z_b$
1.6206°	89.4385°	89.7364°
$\angle y_m x_b$	$\angle y_m y_b$	$\angle y_m z_b$
91.4727°	0°	89.4442°
$\angle z_m x_b$	$\angle z_m y_b$	$\angle z_m z_b$
90.5271°	90.0458°	0°

Finally, the azimuth of magnetic compass can be calculated according to the Eqs. (11), (1)–(3). In addition, compared with the previous calibration methods like the calibration method and ellipsoid fitting algorithm, our error-separation method can obtain M_k independently, indicating the sensitivity factor of the magnetometers can be evaluated.

4. Calibration of accelerometers

The basic principle of both the magnetometer and accelerometer is the same. But, compared with the magnetometer, the accelerometer has an advantage since the magnitude and orientation of the gravitational field is constant regardless of the position of the sensor and the vector sum of the earth magnetic field and the disturbance magnetic field applied on the magnetometer varies when the platform is rotated. The primary errors of accelerometers are bias, scale factor, non-orthogonality and misalignment. There are many methods to calibrate accelerometers [2,6,12,13]. For example, a method called scalar calibration has been used to calibrate accelerometers in various random orientations [2]. But the most common method is the multi-position calibration method, in which the body case is mounted on a precision three-axis table and is rotated to a series of accurately known angles and is positioned in different orientations with respect to the local gravity vector [6]. The number of position is not fixed and can be 6, 16, 18, and so on. Here, 6-postion method was adopted to calibrate accelerometer, taking into account of the existence of three-axis rotating platform with high precision and the perfect cuboid frame of magnetic compasses.

The error model of accelerometers can be expressed in a matrix form as follows:

$$\begin{bmatrix} A_x^b \\ A_y^b \\ A_z^b \end{bmatrix} = (A\_m)_{3\times3} \begin{bmatrix} 1/A\_S_x & 0 & 0 \\ 0 & 1/A\_S_y & 0 \\ 0 & 0 & 1/A\_S_z \end{bmatrix} \begin{bmatrix} A_x - A\_O_x \\ A_y - A\_O_y \\ A_z - A\_O_z \end{bmatrix} = \begin{bmatrix} A_{11} & A_{12} & A_{13} \\ A_{21} & A_{22} & A_{23} \\ A_{31} & A_{32} & A_{33} \end{bmatrix} \begin{bmatrix} A_x \\ A_y \\ A_z \end{bmatrix} + \begin{bmatrix} A_{10} \\ A_{20} \\ A_{30} \end{bmatrix} \tag{12}$$

Table 2
Original outputs of the magnetometers and the corresponding components of the earth magnetic field in the direction of the magnetometer axes.

Original outputs of magnetometers (LSB)			Corresponding components of the earth magnetic field ($\times H_e$)		
x_m axis	y_m axis	z_m axis	x_m axis	y_m axis	z_m axis
2322.1	−1463.7	2061.5	0.581133885	−0.311714521	0.549727789
1511	−2276.6	1338.1	0.333217647	−0.568444314	0.324114417
474.2	−2548.8	278.4	0.015929007	−0.654984285	−0.00708276
−605.8	−2284.5	−779.6	−0.31495187	−0.57126738	−0.337350606
−1438.7	−1516.7	−1589.2	−0.568949492	−0.324231023	−0.590847932
−1741.4	−470.4	−1903.2	−0.66194286	0.004801083	−0.688774977
−1480.4	557.4	−1656	−0.582150548	0.328232947	−0.611205113
−714.2	1329	−912.4	−0.349010089	0.570981616	−0.378639146
358.9	1623.3	131.4	−0.019857817	0.663774052	−0.053188013
1450.4	1352	1197.6	0.313311114	0.578064246	0.279731444
2257.3	585.9	1984.3	0.560892854	0.337815521	0.525767882
2548.9	−218.1	2301.4	0.650585074	0.084439111	0.624685511

Table 3
Sensitivity and bias of the magnetometers.

k_x^m(LSB·H_E^{-1})	k_y^m(LSB·H_E^{-1})	k_z^m(LSB·H_E^{-1})
3269.025	3164.3724	3201.5393
b_x^m (LSB)	b_y^m (LSB)	b_z^m (LSB)
423.2436	−480.5164	301.2213

$$|A| = \sqrt{A_{x1}^2 + A_{y1}^2 + A_{z1}^2} = 1 \tag{13}$$

Where A_{x1}, A_{y1} and A_{z1} are the normalized values of the projection of gravity vector on the axes of body frame. A_x,A_y and A_z are the outputs of three accelerometers, $(A\_m)_{3\times3}$ is the 3×3 misalignment matrix that accounts for the non-orthogonality and misalignment, A_S_i and $A\_O_i(i = x, y, orz)$ are the scale factor and bias, respectively. Twelve calibration parameters were estimated with the least-square method. Then, we can calculate the pitch and roll of case body at arbitrary positions as the followings:

$$Pitch = \theta = \arctan\left(\frac{A_{xl}}{\sqrt{A_{yl}^2 + A_{zl}^2}}\right) \tag{14}$$

$$Roll = \gamma = \arctan\left(\frac{A_{yl}}{A_{zl}}\right) \tag{15}$$

5. Experimental results

The calibration of both magnetometers and accelerometers was accomplished on our three-axis rotating platform based on the fact that the magnitude of the Earth's gravity and indoor magnetic field keeps constant during calibration process. With the error-separation method, the calibration parameters for a triad of magnetometers were also acquired. At first, nine angles between measurement axes of magnetometers and body frame axes can be obtained and was shown in Table 1. At the same time, the declination angle (δ) and inclination angle (ϕ) were also acquired and were equal to 2.7°and 44.1°, respectively. According the above eleven angles, the components of earth magnetic field resulting in the corresponding outputs of magnetometers were calculated when the platform was rotated around the z_p axis to the certain angles and was showed in Table 2, and then, the fitted curves were obtained as shown in Fig. 3. The inset of the zoomed portion in Fig. 3 demonstrated the small deviation of the original outputs from the fitted curves. The sensitivity and bias of magnetometers were inferred from the fitted curve and was shown in Table 3, which means the properties of magnetometers can also assessed during the process calibration. From Table 3, it was deduced that the deviation in the sensitivity of a magnetometer triad was less than 3.5%. Here, it must be mentioned that only several-dozen measurement data are needed in our error-separation methods to acquire the above 11 angle parameters and three fitted curves.

Table 4
Correction parameters for the accelerometer triad.

A_{11}	A_{12}	A_{13}	A_{10}
0.9505	−0.0403	0.0062	−8.0802
A_{21}	A_{22}	A_{23}	A_{20}
0.0073	0.9537	−0.0005	18.4789
A_{31}	A_{32}	A_{33}	A_{30}
−0.0046	0.0001	0.9644	16.8812

12 calibration parameters for accelerometers were obtained with the above six-position method and listed in Table 4. Taking the orientation of the platform as reference, the attitude precision of the magnetic compass was evaluated after calibration. Fig. 4a and b showed the errors between the calculated and real values of pitch and roll angles, respectively. When the pitch (θ) or roll (γ) angles was randomly fixed at 20°, all the angle errors were less than 0.21° with γ changing from −60° to 0 or with γ changing from 0 to 60°, respectively.

According the above calibration parameters and the Eqs. (11), (1)–(3), the heading of magnetic compass can be calculated. The heading errors of magnetic compass were evaluated by mounting the magnetic compass on the platform to keep the x_l axis aligned with the x_p axis and taking the heading of the platform as a reference. Fig. 5 showed the heading error of magnetic compass kept level when the platform was rotated in yaw with several random angles in the range from 0° to 360°. Before calibration, the maximum heading error of magnetic compasses was about 20° and was decreased by about 85% to 3° after the combined bias of magnetometers were eliminated. When the sensitivity of magnetometers was further normalized after the bias elimination, the maximum heading error just had little change to 2.5°. The heading reached the highest precision with the maximum errors about 0.2° if the effects from bias, inconsistent sensitivity and non-orthogonality of a triad of magnetometers were taken into accounted. In addition, the influence of attitude on the heading errors was also investigated when both pitch (γ) and roll (θ) angles were from −60° to 60° and was shown in Fig. 6. With the magnitude of both pitch and roll angles increasing, the heading errors exhibited an increasing trend. But the maximum error in the heading was only about 0.4° even if the magnitude of both pitch and roll angles increased up to 60°. The above experimental results demonstrated that the calibration method of error separation was very effective and efficient to obtain the magnetic compass with high precision of heading. At the same time, the effect of bias, scale factor or non-orthogonality can independently be evaluated. In our magnetic compass, the heading error of our magnetic compass was mainly attributed to the bias of magnetometer, which was consistent with that the sensitivity of a magnetometer triad was close to each other and the deviation

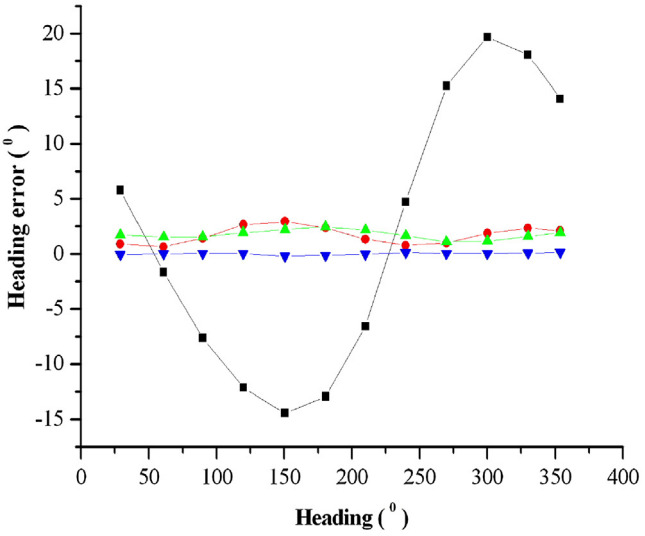

Fig. 5. Heading errors of the magnetic compass in the level state, (■) before calibration; (●) after eliminating the effect of the bias; (▲) after eliminating the effect of the bias and scale factor; (▼) after eliminating the effect of the bias, scale factor and non-orthogonality or misalignment.

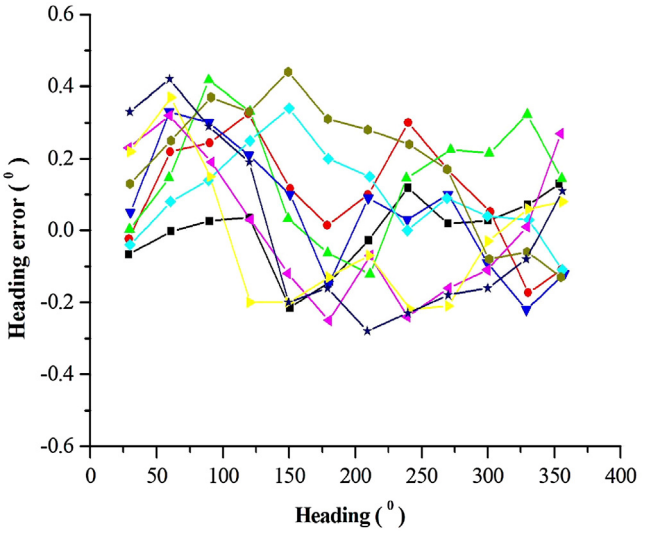

Fig. 6. Heading errors of magnetic compasses with the different attitudes, (■) θ = 0°, γ = 0°; (▲) θ = 30°, γ = 30° and (▼) θ = 30°, γ = −30°; (♦) θ = −30°, γ = 30°; (◀)θ = −30°, γ = −30°; (●) θ = 60°, γ = 60°; (►) θ = 60°, γ = −60°; (●) θ = −60°, γ = 60° and (★) θ = −60°, γ = −60°.

angles between the axe in the measurement frame and the corresponding axe in body frame was very small. But in order to decrease the heading errors as much as possible, the influence from scale factor and non-orthogonality can not be ignored.

In order to further evaluate the effectiveness of the error-separation method for calibrating magnetic compasses, an example in real world application was shown here. The specifically designed compass was combined with the other device (see Fig. 7a). From Fig. 7b, it can be seen that after calibration, the maximum heading error of the single compass in level condition decreased from about 5.6° to about 0.2°. But, the maximum errors was deteriorated to about 3.6° after the compass was combined with the other device, which indicated that the magnetic disturbance was introduced from the other devices and distort the compass output. Then, as expected, the heading precision of the combined compass was improved to about 0.2° again through the further calibration with our error-separation method (see Fig. 7b). Here, it should be

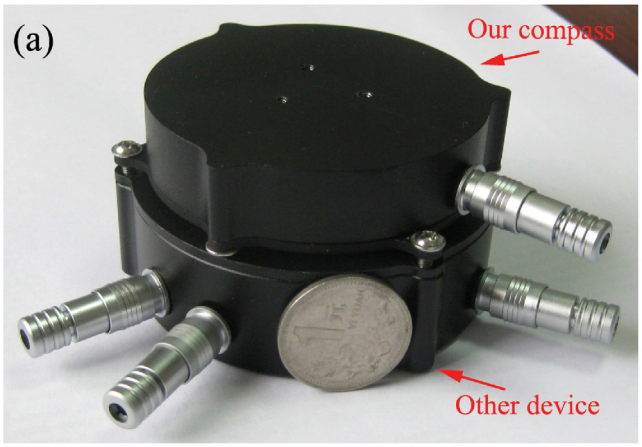

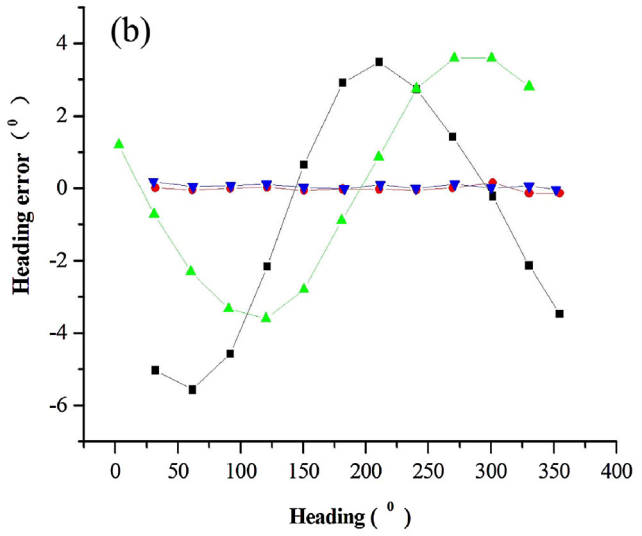

Fig. 7. (a) Photograph of the magnetic compass combined with the other device; (b) Heading errors of the magnetic compass; (■) the single compass before calibration; (●) the single compass after calibration; (▲) the calibrated compass after combined with the other device and (▼) the combined compass after calibration again.

mentioned the common joints and screws in the above devices are purchased from the market. This result demonstrated that our calibration method was also effective to eliminate the magnetic disturbance from the other devices in the real world application and it was not a formidable task to avoid the soft iron interference to the extent that can't distort the output of compasses obviously.

6. Conclusions

A calibration method of error separation based on the self-developed non-magnetic three-axis rotation platform has been proposed and used to calibrate a three-axis magnetic compass consisting of magnetic inductance magnetometers and accelerometers. This calibration method can independently compensate the errors from the non-orthogonality and misalignment, combined bias, or scale factor and roughly evaluate the property of magnetometers. In our magnetic compass, the heading error was mainly attributed to the combined bias from the offset and hard iron interference. After calibration, the maximum error in heading of magnetic compasses was only about 0.4° under the condition of

the magnitude of both the pitch and roll angles equal to 60°. The achievement of magnetic compasses with high heading precision demonstrated that the method of error separation was convenient and effective to calibrate magnetic compasses.

References

[1] M. Sipos, J. Rohac, P. Novacek, Improvement of electronic compass accuracy based on magnetometer and accelerometer calibration, Acta Phys. Polonica A 121 (2012) 945–949.
[2] J. Včelák, P. Ripka, J. Kubík, A. Platil, P. Kašpar, AMR navigation systems and methods of their calibration, Sens. Actuator A 123–124 (2005) 122–128.
[3] M.J. Caruso, Applications of magnetoresistive sensors in navigation systems, SAE Trans. 106 (1997) 1092–1098.
[4] D. Gebre-Egizabher, G.H. Elkaim, J. David Powell, B.W. Parkinson, Calibration of strapdown magnetometers in magnetic field domain, J. Aeros. Eng. 19 (2006) 87–102.
[5] J.H. Wang, Y. Gao, A new magnetic compass calibration algorithm using neural networks, Meas. Sci. Technol. 17 (2006) 153–160.
[6] J.C. Fang, H.W. Sun, J.J. Cao, X. Zhang, Y. Tao, A novel calibration method of magnetic compass based on ellipsoid fitting, IEEE Trans. Instrum. Meas. 60 (2011) 2053–2061.
[7] V. Renaudin, M.H. Afzal, G. Lachapelle, Complete triaxis magnetometer calibration in the magnetic domain, J. Sens. 2010 (2010), 9672452010.
[8] T. Beravs, S. Beguš, J. Podobnik, M. Munih, Magnetometer calibration using Kalman filter covariance matrix for online estimation of magnetic field orientation, IEEE Trans. Instrum. Meas. 63 (2014) 2013–2020.
[9] V. Petrucha, P. Kaspar, P. Ripka, J. Merayo, Automated system for the calibration of magnetometers, J. Appl. Phys. 105 (2009) 07E704.
[10] D. Jurman, M. Jankovec, R. Kamnik, M. Topič, Calibration and data fusion solution for the miniature attitude and heading reference system, Sens. Actuator A 138 (2007) 411–420.
[11] M.J. Caruso, T. Bratland, C.H. Simth, R. Schneider, A new perspective on magnetic field sensing, Sensors (Peterborough, NH) 12 (1998) 15.
[12] A.B. Chatfield, Fundamentals of High Accuracy Inertial Navigation, American Institute of Aeronautics and Astronautics, Reston, Virginia, USA, 1997.
[13] Z.F. Syed, P. Aggarwal, C. Goodall, X. Niu, E. El-Sheimy, A new multi-position calibration method for MEMS inertial navigation systems, Meas. Sci. Technol. 18 (2007) 1897–1907.

Biographies

Zhiwei Chu is currently a MS candidate at Institute of Intelligent Machines, Hefei Institute of Physical Sciences, Chinese Academy of Sciences and Department of Automation, School of Information Science and Technology, University of Science and Technology of China. His research interests include sensors, electronics, signal processing for low-cost precise navigation systems.

Xinhua Lin received the PhD degree in material science and engineering at Shanghai Institute Ceramics, Chinese Academy of Sciences, China in 2003. Now, he is an associate researcher at Institute of Intelligent Machines, Hefei Institute of Physical Sciences, Chinese Academy of Sciences, China. His main research interests are magnetic sensors and magnetic measurements.

Ke Gao is currently a MS candidate at Institute of Intelligent Machines, Hefei Institute of Physical Sciences, Chinese Academy of Sciences and Department of Automation, School of Information Science and Technology, University of Science and Technology of China. His research interests include sensors, electronics, signal processing for low-cost precise navigation systems.

Chenlai Chen received the PhD degree in precision machinery and precision instruments at University of Science and Technology of China in 2011. At present, he is an associate researcher at Institute of Intelligent Machines, Hefei Institute of Physical Sciences, Chinese Academy of Sciences, China. His major interests are devices and instruments for monitoring environment.